6-8-2015

Direct Atmospheric Evidence for the Irreversible Formation Of Aqueous Secondary Organic Aerosol

Marwa M. El-Sayed
University of Maryland at Baltimore, elsayedm@erau.edu

Yingqing Wang
University of Maryland at Baltimore

Christopher J. Hennigan
University of Maryland at Baltimore

Scholarly Commons Citation
El-Sayed, M.M.H.,Y. Wang, and C.J. Hennigan(2015), Direct atmospheric evidence for the irreversible formation of aqueous secondary organic aerosol, Geophys.Res.Lett.,42,5577–5586, doi:10.1002/2015GL064556

AGU PUBLICATIONS

Geophysical Research Letters

RESEARCH LETTER

10.1002/2015GL064556

Key Points:

- WSOCg taken up into aerosol water does not volatilize upon water evaporation
- This demonstrates irreversible aqSOA formation in atmospheric aerosol water
- This has direct implications for interpreting prior laboratory studies of aqSOA

Supporting Information:

- Texts S1–S3, Figures S1–S4, and Tables S1–S4

Correspondence to:
C. J. Hennigan,
hennigan@umbc.edu

Citation:
El-Sayed, M. M. H., Y. Wang, and C. J. Hennigan (2015), Direct atmospheric evidence for the irreversible formation of aqueous secondary organic aerosol, *Geophys. Res. Lett.*, *42*, 5577–5586, doi:10.1002/2015GL064556.

Received 13 MAY 2015
Accepted 5 JUN 2015
Accepted article online 8 JUN 2015
Published online 3 JUL 2015

Direct atmospheric evidence for the irreversible formation of aqueous secondary organic aerosol

Marwa M. H. El-Sayed[1], **Yingqing Wang**[1], **and Christopher J. Hennigan**[1]

[1]Department of Chemical, Biochemical and Environmental Engineering, University of Maryland, Baltimore County, Baltimore, Maryland, USA

Abstract The reversible nature of aqueous secondary organic aerosol (aqSOA) formation was characterized for the first time through direct atmospheric measurements. Water-soluble organic carbon in the gas and particle phases ($WSOC_g$ and $WSOC_p$) was measured simultaneously to quantify aqSOA formation in Baltimore, Maryland. During the nighttime, aqSOA formation was evident as $WSOC_g$ increasingly partitioned to the particle phase with increasing relative humidity (RH). To characterize the reversible/irreversible nature of this aqSOA, the $WSOC_p$ measurement was alternated through an unperturbed ambient channel and through a "dried" channel maintained at ~40% RH (with 7 s residence time) to mimic the natural drying particles undergo throughout the day. Across the entire RH range encountered, there was no statistically significant difference in $WSOC_p$ concentrations through the dry and ambient channels, indicating that the aqSOA remained in the condensed phase upon the evaporation of aerosol water. This strongly suggests that the observed aqSOA was formed irreversibly.

1. Introduction

Recent evidence indicates that the uptake of water-soluble organic gases into atmospheric waters—clouds, fog, and aerosol water—likely represents an important pathway for secondary organic aerosol (SOA) formation [*Ervens et al.*, 2011]. This aqueous SOA (aqSOA) can help to explain the underprediction of SOA concentrations by many state-of-the-art models [*Volkamer et al.*, 2007; *Carlton et al.*, 2008; *Fu et al.*, 2009]; however, fundamental aspects of aqSOA formation remain uncertain or unknown. This includes uncertainties in the relative contributions of reversible and irreversible uptake processes.

Both reversible and irreversible processes are initiated when low carbon number (i.e., volatile), water-soluble organic gases partition to aerosol water or cloud/fog droplets. Once in the aqueous phase, the dissolved organics can undergo various reversible reactions, including hydration and self-reaction to form oligomers [*De Haan et al.*, 2009]. Following these processes, water droplet evaporation can result in a significant loss of the dissolved organics back to the gas phase through repartitioning [*De Haan et al.*, 2009; *Galloway et al.*, 2009], implying that the liquid water serves only as a temporary reservoir for these species. The dissolved organics can also undergo irreversible reactions that form lower volatility products which remain in the condensed phase upon water evaporation. These irreversible reactions are likely driven by radical species [*Anastasio and McGregor*, 2001; *Lim et al.*, 2010; *Ervens et al.*, 2014], inorganics [*Nguyen et al.*, 2012; *Lee et al.*, 2013; *Ortiz-Montalvo et al.*, 2014], and acid catalysis [*Surratt et al.*, 2007; *Gaston et al.*, 2014]. The relative split between the reversible and irreversible pathways is an important factor that influences the contribution of aqSOA to the total OA budget [*De Haan et al.*, 2009].

Due to its high solubility in water and numerous atmospheric sources, glyoxal is thought to be a dominant aqSOA precursor [*Volkamer et al.*, 2007; *McNeill et al.*, 2012; *Lin et al.*, 2014]. Consequently, glyoxal has been investigated extensively in laboratory and modeling studies. Reversible glyoxal uptake to aqueous particles readily forms significant concentrations of aqSOA [e.g., *Kroll et al.*, 2005; *Galloway et al.*, 2009]. Glyoxal is also highly reactive in the aqueous phase [e.g., *Carlton et al.*, 2007; *Shapiro et al.*, 2009; *Yu et al.*, 2011], indicating that it is very likely to undergo irreversible uptake [*Lim et al.*, 2010; *Ervens and Volkamer*, 2010]. Methylglyoxal is far less soluble than glyoxal and is unlikely to contribute significant aqSOA through reversible uptake to fine-particle water [*Kroll et al.*, 2005]. However, due to far-greater liquid water content in clouds than wet aerosols, the reversible uptake of methylglyoxal and subsequent repartitioning to the gas phase through cloud cycles is predicted [*Lim et al.*, 2013]. Methylglyoxal is also highly reactive in the aqueous phase (e.g., with OH and inorganics) [*Altieri et al.*, 2008; *Sareen et al.*, 2010], which would imply irreversible uptake in both fine-particle water and cloud/fog droplets. It is thus thought to be an important precursor to aqSOA of similar or greater magnitude to glyoxal [*Fu et al.*, 2008; *Lin et al.*, 2012]. The reaction products of isoprene oxidation, specifically epoxides of isoprene (IEPOX), have also been identified as major aqSOA precursors [*Paulot et al.*, 2009; *Lin et al.*, 2012; *McNeill et al.*, 2012; *Pye et al.*, 2013]. The uptake is thought to proceed through reversible Henry's law partitioning with a subsequent aqueous-phase mechanism that includes ring opening and nucleophilic addition catalyzed by a proton donor [*T. B. Nguyen et al.*, 2014; *Gaston et al.*, 2014]. A recent study indicates that ~5–25% of the IEPOX taken up by particles ultimately forms SOA, suggesting that a majority of the uptake is reversible [*Riedel et al.*, 2015]. However, *T. B. Nguyen et al.* [2014] showed that inorganic seed particle composition quite strongly affects this process.

Since most clouds are not precipitating [*Pruppacher*, 1986] and because aerosol water levels can change widely with changes in aerosol composition and relative humidity (RH) [*Khlystov et al.*, 2005; *T. K. Nguyen et al.*, 2014], understanding the fate of aqSOA under conditions of water evaporation is critical in quantifying the contribution of aqSOA to the total OA budget. For glyoxal dissolved in water or taken up through a reversible process, dilution of the system with clean air or evaporation of the liquid droplets causes glyoxal to repartition to the gas phase, demonstrating the reversible nature of the uptake [*De Haan et al.*, 2009; *Galloway et al.*, 2009; *Ortiz-Montalvo et al.*, 2012]. However, not all of the glyoxal volatilizes: some remains in the condensed phase upon water droplet evaporation [*Loeffler et al.*, 2006; *De Haan et al.*, 2009; *Galloway et al.*, 2014]. Substantial organic mass remains in the condensed phase upon evaporation of aqueous droplets containing dissolved methylglyoxal as well [*De Haan et al.*, 2009; *Galloway et al.*, 2014]. In the absence of inorganic species, this behavior is attributed to the formation of lower volatility oligomers [*Loeffler et al.*, 2006; *De Haan et al.*, 2009]. The behavior of β-IEPOX SOA upon aerosol water evaporation is a function of the inorganic aerosol seed. For example, in experiments of β-IEPOX uptake to aqueous NaCl particles, the observed aqSOA completely evaporated under conditions of aerosol water drying, indicating reversible aqSOA formation [*T. B. Nguyen et al.*, 2014]. Conversely, significant aqSOA remained in the condensed phase under conditions of aerosol water drying when the β-IEPOX uptake occurred on aqueous $(NH_4)_2SO_4$ particles [*T. B. Nguyen et al.*, 2014].

Experimental evidence suggests that particle water evaporation can also induce or rapidly accelerate chemical reactions compared to conditions in the bulk aqueous phase. The presence of ammonium may be especially key for such processes as it can dramatically alter the quantity and composition of organics that remain in the condensed phase under conditions of evaporation [*De Haan et al.*, 2011; *Nguyen et al.*, 2012; *Lee et al.*, 2013; *Yli-Juuti et al.*, 2013; *Ortiz-Montalvo et al.*, 2014].

What remains mostly unknown is how these experimental observations translate into ambient aqSOA formation. A major challenge is that organic and inorganic matrix effects have a profound impact on the chemistry of organic compounds in bulk aqueous solutions, aqueous particles, and in particles undergoing drying [*Volkamer et al.*, 2009; *Tan et al.*, 2009; *Laskin et al.*, 2012; *Drozd and McNeill*, 2014; *Powelson et al.*, 2014; *Ortiz-Montalvo et al.*, 2014]. This includes the potentially important effects of both liquid-liquid phase separations [*You et al.*, 2012] and changes in organic particle viscosity [*Song et al.*, 2015] under conditions of aerosol water evaporation. However, the effect of either process on SOA formed through the uptake of water-soluble gases to aqueous particles is unknown at present.

The purpose of this study was to characterize the reversible nature of aqSOA formation through direct atmospheric observations. A central component of this study was an analysis of the behavior of particulate water-soluble organic carbon ($WSOC_p$) under conditions of aerosol drying. Ambient measurements were carried out for approximately 1 month in Baltimore, Maryland, a site heavily impacted by anthropogenic and biogenic emissions. Two main SOA formation processes were identified as follows: (1) daytime photochemical SOA production and (2) nighttime partitioning of water-soluble organic carbon from the gas phase ($WSOC_g$) to particle phase ($WSOC_p$) at enhanced relative humidity (RH) (i.e., aqSOA formation). We focus on comparing the behavior of $WSOC_p$, a surrogate for SOA, in dried/ambient particles under these two SOA formation regimes. This represents, to our knowledge, the first attempt to quantify and differentiate reversible and irreversible aqSOA in the atmosphere.

2. Methods

Ambient measurements were carried out in Baltimore, Maryland, from 3–30 September 2014 on the University of Maryland, Baltimore County (UMBC) campus. The measurements included $WSOC_p$ and $WSOC_g$, total aerosol organic and elemental carbon (OC and EC, Sunset Labs Field Analyzer), and carbon monoxide (CO, Thermo Scientific Model 48C). Instrumentation was housed in a temperature-controlled environmental enclosure (EKTO, Inc.) located on the rooftop of the Engineering Building at UMBC. The rooftop is ~20 m above ground level, and the air sampling inlets were ~3 m above the rooftop.

A detailed description of all methods, including a schematic of the experimental setup (Figure S1), is included in the supporting information. Briefly, online measurements of $WSOC_p$ were made with a Particle-into-Liquid Sampler (PILS, Brechtel Manufacturing) coupled to a Total Organic Carbon Analyzer (TOC, Model 900 Turbo, GE Analytical) operated in Turbo mode according to the method of *Sullivan et al.* [2006]. The $WSOC_p$ measurements employed a $PM_{2.5}$ cyclone (URG Corp.) and a parallel plate carbon denuder to remove any interference from organic vapors. The $WSOC_g$ measurements were carried out with a mist chamber (MC) coupled to the same TOC analyzer according to the method of *Hennigan et al.* [2008, 2009]. The mist chamber was operated with 10 mL initial water collection volume, with an air sample flow rate of 28.2 l min^{-1}, and 5 min sample collection times.

To characterize the effect of aerosol water evaporation on aqSOA, the $WSOC_p$ sample was alternated between an unperturbed ambient channel and a "dried" channel in which the air sample passed through a silica gel dryer. The measurement through the ambient channel is denoted as "$WSOC_p$" while that through the dried channel is denoted "$WSOC_{p,dry}$." The dryer was made in-house, similar to other commercial models (e.g., TSI model 3062), and had a 4 s residence time. Under the present experimental conditions and across the ambient temperature (*T*) and relative humidity (RH) encountered in September, the air sample exiting the dryer had an average RH of 42.5% ± 0.9% (range = 33.7–45.9%; supporting information Table S1). The dryer was exchanged daily, and its continued efficiency at the end of the 1 day sampling was confirmed with both color indicator of the silica gel and direct laboratory measurements (Omega, RH-USB). Under both the ambient and dried $WSOC_p$ measurement configurations, the air sample passed through the parallel plate denuder prior to the PILS; thus, any organic aerosol species that evaporated downstream of the dryer (i.e., due to particle water evaporation) were also removed, avoiding recondensation in the PILS. The $WSOC_p$ measurement was modulated between the dry and ambient channels using an automated three-way stainless steel valve (Brechtel Manufacturing). Particle losses through the three-way valve and dryer were characterized prior to the study and were negligible. Particle sizing measurements were not undertaken as part of this study, so a quantitative comparison of the aerosol water content in the respective channels was not possible. Qualitatively, the decrease in RH from ambient down to ~40% will substantially reduce the aerosol liquid water content for most ambient aerosol compositions, especially when the ambient RH is above 80% [*Malm and Day*, 2001]. The dryer + carbon denuder provided a 7 s residence time for the dried sample at the decreased RH prior to particle collection in the PILS. This amount of time far exceeds the required time for aerosol water evaporation, which is of order 10^{-3} s for fine particles [*Hinds*, 1999], but may not allow complete evaporation of condensed organics, depending on many factors, including the organic aerosol matrix. The implications of this timing are discussed in detail below.

A single $WSOC_g$-$WSOC_p$-$WSOC_{p,dry}$ cycle was completed every 14 min. A syringe pump (C3000, Tricontinent Scientific) and peristaltic pump (Ismatec) were used in conjunction with an eight-port distribution valve (Valco) to alternately deliver the $WSOC_p$ sample (5 min), the $WSOC_{p,dry}$ sample (5 min), and the $WSOC_g$ sample (4 min) to the TOC analyzer. Data from the TOC analyzer operated in turbo mode were averaged to provide one measurement each of $WSOC_g$, $WSOC_p$, and $WSOC_{p,dry}$ every 14 min cycle. Factory calibrations of the TOC analyzer were performed, and these calibrations were periodically verified using sucrose solutions with concentrations that bracketed our observed aqueous sample concentrations. Dynamic blanks for the PILS and MC systems were measured approximately daily, and were subtracted from the ambient measurements to properly quantify the $WSOC_g$ and $WSOC_p$ concentrations. The dynamic blanks were also used to quantify the method limits of detection, which were 0.23 and 0.35 μg-C m^{-3} for $WSOC_p$ and $WSOC_g$, respectively.

No direct measurement of SOA exists, but $WSOC_p$ is a good surrogate for SOA in most environments [e.g., *Miyazaki et al.*, 2006; *Kondo et al.*, 2007; *Weber et al.*, 2007]. $WSOC_g$ represents a bulk measurement of oxygenated organic gases, which are predominantly secondary, as well [*Hennigan et al.*, 2009; *Carlton and Turpin*, 2013; *Hodzic et al.*, 2014; *Yuan et al.*, 2015]. The production of gas- and particle-phase WSOC was

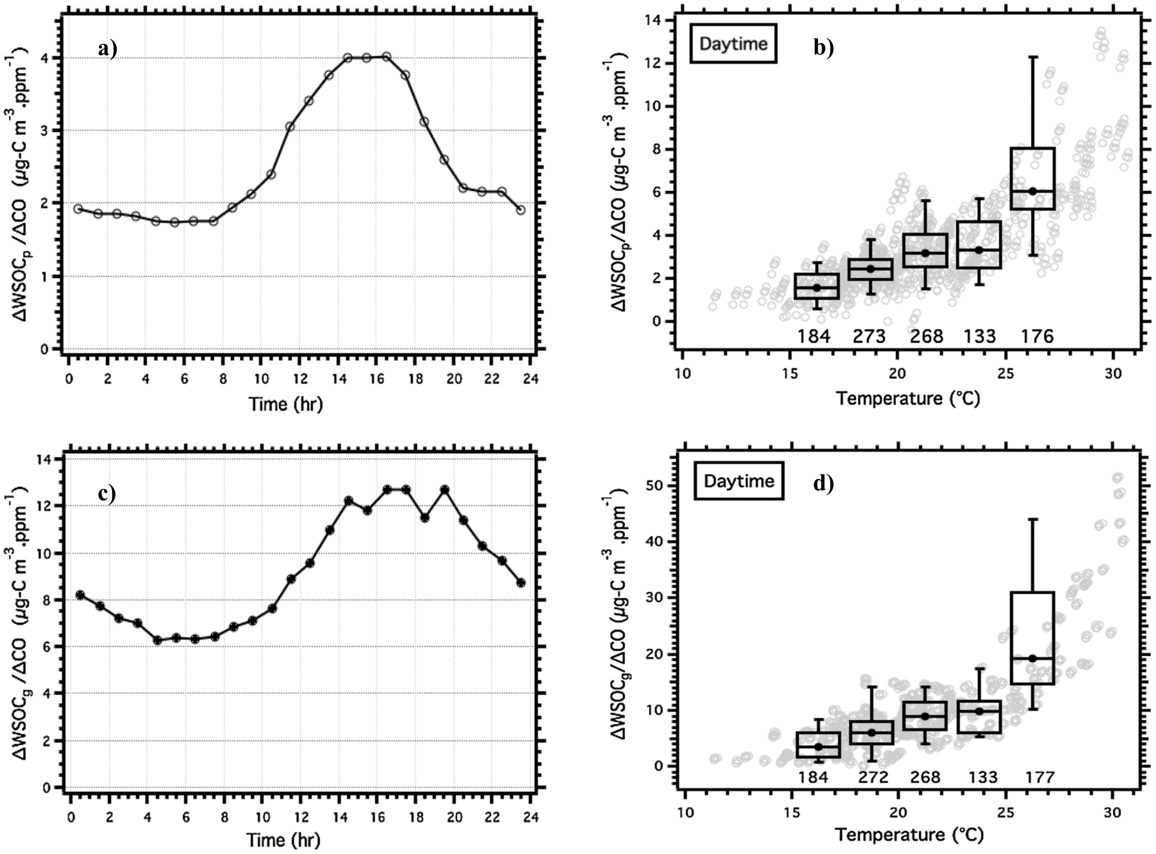

Figure 1. Average diurnal profiles of (a) $\Delta WSOC_p/\Delta CO$ and (c) $\Delta WSOC_g/\Delta CO$. Boxplots of (b) $\Delta WSOC_p/\Delta CO$ and (d) $\Delta WSOC_g/\Delta CO$ as a function of temperature. Data were binned according to the ambient temperature: bins were defined as 10–17.5°C, 17.5–20°C, 20–22.5°C, 22.5–25°C, and 25–35°C. For each bin, median values (horizontal line with dot), 25th and 75th percentiles (lower and upper box values), and 5th and 95th percentiles (vertical lines) are shown. The numbers at the bottom of Figures 1b and 1d represent the number of points within each bin.

quantified by normalizing the excess WSOC concentrations (ΔWSOC) to the excess CO concentration (ΔCO). This method accounts for dilution due to boundary layer expansion and for the mixing of different air masses sampled at the ground site [*de Gouw et al.*, 2005; *DeCarlo et al.*, 2008; *Zhang et al.*, 2012]. The background concentrations of WSOC and CO were subtracted from each ambient measurement to compute the excess concentrations ($\Delta WSOC_g$, $\Delta WSOC_p$, and ΔCO). The WSOC backgrounds were taken to be the lowest concentrations measured throughout the study (Table S2), while that for CO was assumed to be 0.1 ppm (sixth lowest CO concentration among 3800 measurements in the study period).

3. Results and Discussion

An overview of the $WSOC_g$ and $WSOC_p$ measurements from the entire study period is summarized in the supporting information Table S2. Overall, conditions during the measurement period were relatively clean, due to synoptic conditions that prevented the buildup of pollutants over multiple days. However, SOA formation was consistently observed and was due primarily to two different pathways: (1) daytime photochemical SOA production and (2) nighttime partitioning of $WSOC_g$ to aerosol water (i.e., aqSOA production).

Figures 1a and 1c show the average diurnal profiles of the $\Delta WSOC_p/\Delta CO$ and $\Delta WSOC_g/\Delta CO$ ratios, respectively. The figures show strong photochemical production of $WSOC_p$ and $WSOC_g$, as the normalized concentrations approximately double from 08:00 to 14:00 (local time). It is likely that most of this SOA production is from biogenic VOCs: the summertime VOC budget in the region is dominated by isoprene [*Hudman et al.*, 2008], and isoprene emissions remain relatively high through September in the eastern U.S. [*Müller et al.*, 2008]. This is strongly supported by Figures 1b and 1d, which show large increases in the daytime (08:00–19:00, local time) $\Delta WSOC_p/\Delta CO$ and $\Delta WSOC_g/\Delta CO$ ratios with increasing temperature. This is likely due to the combination of enhanced isoprene emissions, increased oxidant concentrations, and faster kinetics all contributing to SOA production at higher temperatures. The normalized WSOC concentrations also showed a positive relationship with temperature during nighttime periods (20:00 to 07:00 local time, supporting information Figure S2).

During nighttime periods, another SOA formation pathway was prominent: the uptake of $WSOC_g$ to fine-particle water (i.e., forming aqSOA). During the night, the fraction of total WSOC in the particle phase ($F_p = WSOC_p/(WSOC_p + WSOC_g)$) exhibits a statistically significant increasing trend with RH (Figure 2a), with periods of strong correlation (Figures 2b and S4). Other factors besides RH will also influence F_p (e.g., local emissions and SOA formation by other pathways), which explains the scatter in the individual data points in Figure 2a. At the highest RH levels (>80%), the median F_p increased by approximately 50% compared to the median nighttime F_p at the lowest RH levels. The Student's *t* test indicates that the F_p increases at the two highest RH levels (70–80%; > 80% RH) are statistically significant at the 95% confidence level compared to nighttime F_p values at RH < 60% (the increase in F_p for the 60–70% RH bin was not statistically significant). Further, we have identified multiple time periods, where F_p and RH increased simultaneously—one example is shown in Figure 2b, while several more are presented in the supporting information (Figure S4). The observation of nighttime aqSOA formation is further supported by the findings in Figures 1 and S2. Given the lower isoprene and oxidant concentrations at night, one may expect increasing F_p with increasing RH during this time simply due to the enhanced particle-phase partitioning of semivolatile compounds at lower *T* (higher RH). However, the increasing normalized

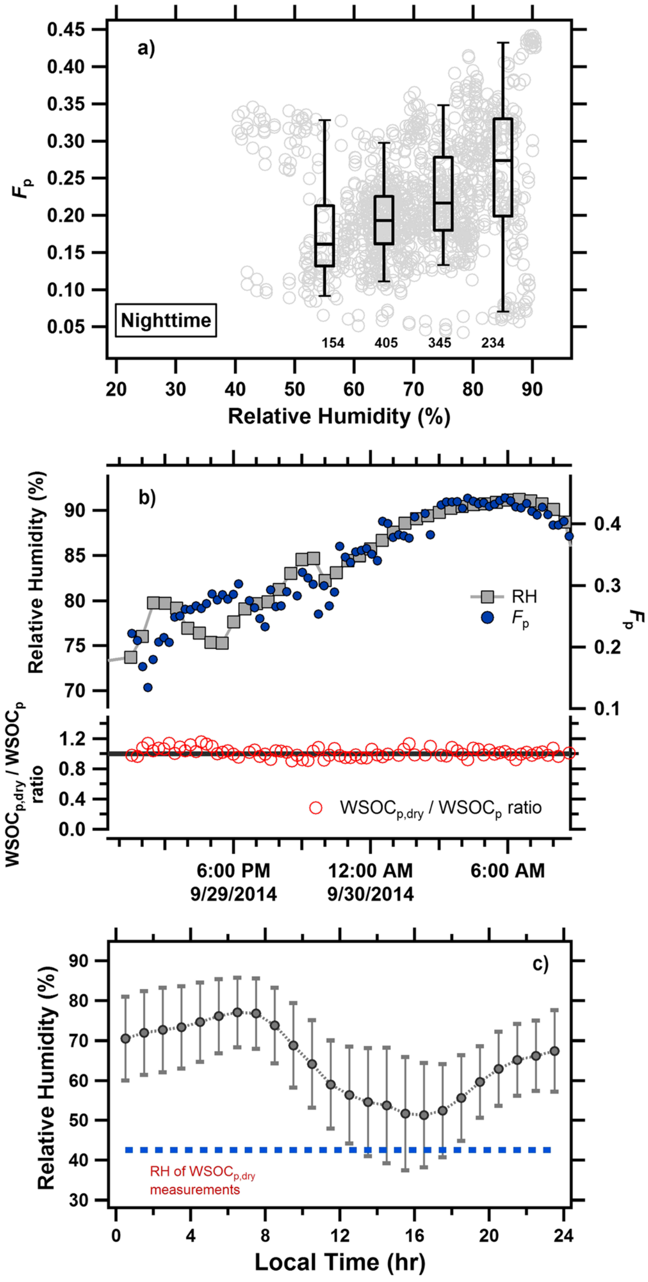

Figure 2. (a) Scatterplot and box plot of the particulate WSOC fraction, F_p, as a function of RH at nighttime (20:00 to 07:00, local time). Data were binned according to the ambient RH: bins were defined as 40–60%, 60–70%, 70–80%, and 80–90%. For each bin, median values (horizontal line), 25th and 75th percentiles (lower and upper box values), and 5th and 95th percentiles (vertical lines) are shown. Numbers at the bottom of Figure 2a represent the number of points within each bin. (b) Event beginning on 29 September 2014 in which F_p and RH increased together while the $WSOC_{p,dry}/WSOC_p$ ratio remained approximately constant. The black solid line at $WSOC_{p,dry}/WSOC_p$ ratio = 1 is for visual reference. (c) Average diurnal profile of RH (vertical bars represent ±1σ). The dotted line at 42.5% RH represents the average RH conditions for the $WSOC_{p,dry}$ measurement.

$WSOC_p$ concentration with increasing temperature at night (Figure S2) shows that other factors, including RH, also affect the concentrations and partitioning of WSOC.

Similar RH dependences to Figure 2 have been observed in other locations as well [*Hennigan et al.*, 2008; *Sorooshian et al.*, 2010; *Zhang et al.*, 2012]. The dark uptake of water-soluble organic gases (e.g., glyoxal) to aerosol water has been observed in both laboratory [e.g., *Liggio et al.*, 2005a; 2005b; *Kroll et al.*, 2005; *Galloway et al.*, 2009; *T. B. Nguyen et al.*, 2014] and ambient studies [*Hennigan et al.*, 2008] and is responsible for the behavior shown in Figure 2a. An overall increase in F_p with increasing RH was not observed during daytime hours (08:00–19:00, Supporting Information Figure S3), suggesting that daytime uptake of $WSOC_g$ to fine-particle water was obscured by the formation of SOA through the emission and photooxidation of VOCs through more traditional gas-phase pathways. Further, of the individual events corresponding to increases in F_p and RH, the majority were observed during nighttime periods, possibly due to lower availability of aerosol water during the daytime.

While this study and others have observed aqSOA formation through the uptake of $WSOC_g$ to aerosol water, a major question that remains is whether this uptake occurs in the atmosphere through reversible or irreversible pathways, since both processes are observed in laboratory studies [*McNeill*, 2015]. To investigate this question, the $WSOC_p$ measurement was modulated between the ambient and dried channels. The RH of the sample through the dried channel was approximately 42.5% (see supporting information Table S1). This level of drying would induce significant aerosol water evaporation, but there was still likely to be residual water associated with many particles at this RH [*Khlystov et al.*, 2005]. The goal was *not* to dry the particles completely but rather to provide an estimate for the lowest RH that particles may encounter naturally over

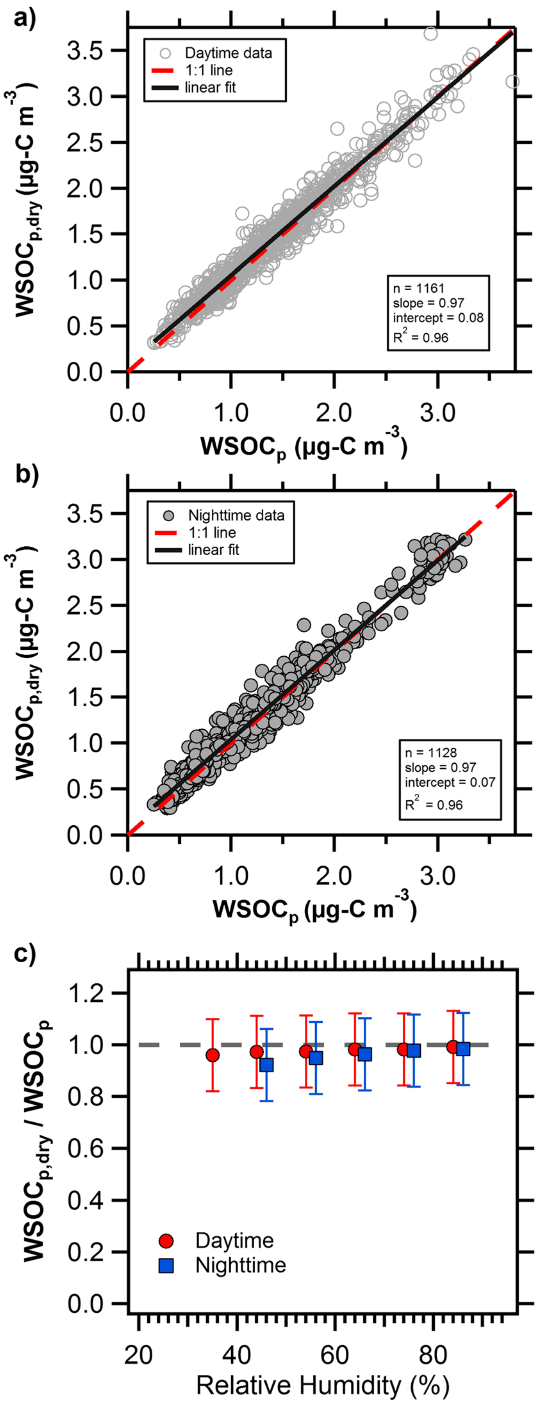

Figure 3. Scatterplots of $WSOC_{p,dry}$ versus $WSOC_p$ for (a) daytime and (b) nighttime periods. The solid black lines in Figures 3a and 3b represent the linear fits to the data using least squares regression analysis; the fit parameters are given in each panel. (c) Median daytime and nighttime values of the $WSOC_{p,dry}/WSOC_p$ ratio as a function of ambient RH. To calculate the $WSOC_{p,dry}/WSOC_p$ ratio, 0.075 µg C m^{-3} was subtracted from each $WSOC_{p,dry}$ measurement to account for the small positive intercept in Figures 3a and 3b. Vertical lines in Figure 3c represent the uncertainty of the calculated WSOC ratio, assuming a relative measurement uncertainty of 10% in both the $WSOC_p$ and $WSOC_{p,dry}$ measurements.

the course of a day in the study period. Figure 2c shows the average daily RH profile (±1σ), along with the average dried sample RH (blue dotted line). This demonstrates that the RH through the dryer provided a reasonable approximation for the low end of RH values across a daily cycle during the study period.

Figure 3 shows a comparison of the $\mathrm{WSOC_p}$ and $\mathrm{WSOC_{p,dry}}$ concentrations for daytime and nighttime periods throughout the study. The slopes very close to unity and low-intercept values in Figures 3a and 3b indicate the strong similarity in the $\mathrm{WSOC_p}$ and $\mathrm{WSOC_{p,dry}}$ concentrations during both daytime and nighttime periods. Figure 3c shows the $\mathrm{WSOC_{p,dry}/WSOC_p}$ ratio for daytime and nighttime periods as a function of ambient RH. Although Figure 3 suggests a small systematic difference between the $\mathrm{WSOC_p}$ and $\mathrm{WSOC_{p,dry}}$ measurements—e.g., the small intercepts or the $\mathrm{WSOC_{p,dry}/WSOC_p}$ ratio slightly below unity—these differences were not statistically significant at any RH level in either the daytime or nighttime periods (supporting information Tables S3 and S4). Figure 3c demonstrates the nearly constant $\mathrm{WSOC_{p,dry}/WSOC_p}$ ratio across the entire RH range. This is supported by Figure 2b, which shows a single event where F_p increased simultaneously with RH. Throughout this event, the $\mathrm{WSOC_{p,dry}/WSOC_p}$ ratio remained approximately constant (average = 1.02). There are several important observations to note from Figure 3. First, aerosol liquid water increases with increasing RH, so the trend in Figure 3c indicates that the evaporation of liquid water had no effect on $\mathrm{WSOC_p}$. Second, there was no difference in the $\mathrm{WSOC_{p,dry}/WSOC_p}$ ratio for the daytime or nighttime periods. This suggests that the $\mathrm{WSOC_p}$ (i.e., SOA) remained in the condensed phase with liquid water evaporation, regardless of the pathway by which the SOA formation occurred (daytime, photochemical gas-phase SOA and nighttime, aqSOA formation in aerosol water).

This study represents, to our knowledge, the first characterization of the reversibility of ambient aqSOA formation. The implication of this work is that aqSOA formed through aerosol liquid water remains in the condensed phase upon evaporation of the water. It is significant that this observation pertains to aqSOA formed under dark conditions. This suggests that OH was not likely responsible for driving aqueous-phase reactions to transform the dissolved $\mathrm{WSOC_p}$. Other compounds, including radicals and inorganic species, may have initiated the chemical transformation of the aqSOA into lower volatility material that remains in the condensed phase upon liquid water evaporation. This includes the formation of organic acid-salt complexes [*Laskin et al.*, 2012; *Wang and Laskin*, 2014], which can dramatically decrease the vapor pressure of organic compounds [*Paciga et al.*, 2014].

It is also possible that self-reactions to form oligomers contributed to the aqueous-phase chemistry, although this was not likely the primary reaction mechanism, since some $\mathrm{WSOC_p}$ evaporation along with the liquid water would be expected if that were the case [*De Haan et al.*, 2009; *Ortiz-Montalvo et al.*, 2012]. The effects of both liquid-liquid phase separations and changing organic component viscosities under conditions of particle water evaporation may contribute to the ambient observations. Laboratory experiments indicate that biogenic SOA under high-RH conditions (>80%) is almost certainly in the liquid phase [*Renbaum-Wolff et al.*, 2013; *Song et al.*, 2015]. The same experiments also observed significant increases in SOA viscosities when RH levels were decreased. *Galloway et al.* [2014] hypothesized that oligomer formation in model aqSOA particles undergoing drying increased the particle viscosities and inhibited the complete evaporation of aerosol water. Although the above studies suggest that the viscosity of SOA likely changed in our "dry" channel, it cannot be determined from the present measurements whether this effect was indeed responsible for the lack of $\mathrm{WSOC_p}$ evaporation under the conditions of drying. Predicting the effects of changing aerosol phase on the observed results is further complicated by the variable influence of inorganic species and organic aerosol composition (e.g., O:C ratio) on aerosol water and phase state [*Hodas et al.*, 2015].

The results in this study have characterized the behavior of aqSOA formed through aerosol water under conditions of liquid water evaporation. However, the translation of these results to aqSOA formed in cloud water is uncertain. The aqueous chemistry in aerosol and cloud water is likely to be quite different due to wide differences in liquid water content and solute concentrations [*Tan et al.*, 2009; *Ervens and Volkamer*, 2010]. The fate of dissolved organic species under water droplet evaporation as a function of initial organic concentrations has not been systematically investigated. Further, matrix effects can significantly alter the aqueous chemistry of organics [*Drozd and McNeill*, 2014], so the methods used in this study should be deployed in diverse locations and across multiple seasons to characterize a wider range in meteorology, source influences, and aerosol composition. Finally, the kinetics of evaporation was not assessed in this study, but the delayed evaporation of semivolatile $\mathrm{WSOC_p}$ cannot be ruled out. The total residence time for the $\mathrm{WSOC_{p,dry}}$ channel within and downstream of the silica gel dryer prior to particle collection in the

PILS was ~7 s. This includes the residence time in the parallel plate carbon denuder. This timing is similar to the evaporation times used by *T. B. Nguyen et al*. [2014] (~3–4 s) and *Ortiz-Montalvo et al*. [2012, 2014] (6 s) to investigate aqSOA behavior in evaporating aqueous particles in laboratory studies. This amount of time is more than sufficient to allow aerosol water evaporation, which occurs on a time scale of ~10^{-3} s in fine particles [*Hinds*, 1999]. Laboratory studies and thermodynamic models suggest that 7 s may or may not be sufficient to reach equilibrium in evaporating water/organic droplets, though, depending on the droplet composition. For example, *T. B. Nguyen et al*. [2014] observed the complete evaporation of aqSOA formed from β-IEPOX uptake to aqueous NaCl particles that underwent drying for 3–4 s. Conversely, *Yli-Juuti et al*. [2013] found required drying times in excess of 20 s for mixed succinic acid-ammonium sulfate particles, while *Galloway et al*. [2014] found equilibrium drying times of up to 2 min for aqueous carbonyl-ammonium sulfate particles. Nevertheless, if $WSOC_p$ evaporation were to occur as a result of the aerosol water evaporation, the 7 s residence time would be sufficient to allow some of the $WSOC_p$ evaporation to occur [*Yli-Juuti et al*., 2013; *Galloway et al*., 2014]. The fact that we observed no statistical difference between the $WSOC_p$ and $WSOC_{p,dry}$ measurements suggests that all of the observed aqSOA was irreversible.

Overall, we have demonstrated evidence for the irreversible formation of aqSOA in fine-particle water in the atmosphere. The $WSOC_g$ that partitioned to aerosol water at elevated RH remained in the condensed phase upon evaporation of the water. This characterization was predominantly under dark conditions, indicating that aqueous reactions of the dissolved organics with OH are not necessary to form irreversible aqSOA. This study reinforces the importance of aqueous pathways as contributors to ambient SOA [*Ervens et al*., 2011; *McNeill*, 2015], although significant work remains in quantifying the contribution of aqueous pathways to the global OA burden.

Acknowledgments
The authors gratefully acknowledge the use of meteorology data from Joshua Cole and Claire Welty of UMBC's Center for Urban Environmental Research and Education. The data used in this analysis are available upon request. This work was supported by the National Science Foundation through award AGS-1464458.

The Editor thanks two anonymous reviewers for their assistance in evaluating this paper.

References

Altieri, K. E., S. P. Seitzinger, A. G. Carlton, B. J. Turpin, G. C. Klein, and A. G. Marshall (2008), Oligomers formed through in-cloud methylglyoxal reactions: Chemical composition, properties, and mechanisms investigated by ultra-high resolution FT-ICR mass spectrometry, *Atmos. Environ.*, *42*(7), 1476–1490, doi:10.1016/j.atmosenv.2007.11.015.

Anastasio, C., and K. G. McGregor (2001), Chemistry of fog waters in California's Central Valley: 1. In situ photoformation of hydroxyl radical and singlet molecular oxygen, *Atmos. Environ.*, *35*(6), 1079–1089, doi:10.1016/S1352-2310(00)00281-8.

Carlton, A. G., and B. J. Turpin (2013), Particle partitioning potential of organic compounds is highest in the Eastern US and driven by anthropogenic water, *Atmos. Chem. Phys.*, *13*(20), 10,203–10,214, doi:10.5194/acp-13-10203-2013.

Carlton, A. G., B. J. Turpin, K. E. Altieri, S. Seitzinger, A. Reff, H. J. Lim, and B. Ervens (2007), Atmospheric oxalic acid and SOA production from glyoxal: Results of aqueous photooxidation experiments, *Atmos. Environ.*, *41*(35), 7588–7602, doi:10.1016/j.atmosenv.2007.05.035.

Carlton, A. G., B. J. Turpin, K. E. Altieri, S. P. Seitzinger, R. Mathur, S. J. Roselle, and R. J. Weber (2008), CMAQ model performance enhanced when in-cloud secondary organic aerosol is included: Comparisons of organic carbon predictions with measurements, *Environ. Sci. Technol.*, *42*(23), 8798–8802, doi:10.1021/Es801192n.

de Gouw, J. A., et al. (2005), Budget of organic carbon in a polluted atmosphere: Results from the New England Air Quality Study in 2002, *J. Geophys. Res.*, *110*(D16), 1984–2012, doi:10.1029/2004JD005623.

De Haan, D. O., A. L. Corrigan, M. A. Tolbert, J. L. Jimenez, S. E. Wood, and J. J. Turley (2009), Secondary organic aerosol formation by self-reactions of methylglyoxal and glyoxal in evaporating droplets, *Environ. Sci. Technol.*, *43*(21), 8184–8190, doi:10.1021/Es902152t.

De Haan, D. O., L. N. Hawkins, J. A. Kononenko, J. J. Turley, A. L. Corrigan, M. A. Tolbert, and J. L. Jimenez (2011), Formation of nitrogen-containing oligomers by methylglyoxal and amines in simulated evaporating cloud droplets, *Environ. Sci. Technol.*, *45*(3), 984–991, doi:10.1021/es102933x.

DeCarlo, P. F., et al. (2008), Fast airborne aerosol size and chemistry measurements above Mexico City and Central Mexico during the MILAGRO campaign, *Atmos. Chem. Phys.*, *8*(14), 4027–4048, doi:10.5194/acp-8-4027-2008.

Drozd, G. T., and V. F. McNeill (2014), Organic matrix effects on the formation of light-absorbing compounds from α-dicarbonyls in aqueous salt solution, *Environ. Sci. Processes Impacts*, *16*(4), 741–747, doi:10.1039/C3EM00579H.

Ervens, B., and R. Volkamer (2010), Glyoxal processing by aerosol multiphase chemistry: Towards a kinetic modeling framework of secondary organic aerosol formation in aqueous particles, *Atmos. Chem. Phys.*, *10*(17), 8219–8244, doi:10.5194/acp-10-8219-2010.

Ervens, B., B. J. Turpin, and R. J. Weber (2011), Secondary organic aerosol formation in cloud droplets and aqueous particles (aqSOA): A review of laboratory, field and model studies, *Atmos. Chem. Phys.*, *11*(21), 11,069–11,102, doi:10.5194/acp-11-11069-2011.

Ervens, B., A. Sorooshian, Y. B. Lim, and B. J. Turpin (2014), Key parameters controlling OH-initiated formation of secondary organic aerosol in the aqueous phase (aqSOA), *J. Geophys. Res. Atmos.*, *119*, 3997–4016, doi:10.1002/2013JD021021.

Fu, T. M., D. J. Jacob, F. Wittrock, J. P. Burrows, M. Vrekoussis, and D. K. Henze (2008), Global budgets of atmospheric glyoxal and methylglyoxal, and implications for formation of secondary organic aerosols, *J. Geophys. Res.*, *113*, D15303, doi:10.1029/2007JD009505.

Fu, T. M., D. J. Jacob, and C. L. Heald (2009), Aqueous-phase reactive uptake of dicarbonyls as a source of organic aerosol over eastern North America, *Atmos. Environ.*, *43*(10), 1814–1822, doi:10.1016/j.atmosenv.2008.12.029.

Galloway, M. M., P. S. Chhabra, A. W. H. Chan, J. D. Surratt, R. C. Flagan, J. H. Seinfeld, and F. N. Keutsch (2009), Glyoxal uptake on ammonium sulphate seed aerosol: Reaction products and reversibility of uptake under dark and irradiated conditions, *Atmos. Chem. Phys.*, *9*(10), 3331–3345, doi:10.5194/acp-9-3331-2009.

Galloway, M. M., M. H. Powelson, N. Sedehi, S. E. Wood, K. D. Millage, J. A. Kononenko, A. D. Rynaski, and D. O. De Haan (2014), Secondary organic aerosol formation during evaporation of droplets containing atmospheric aldehydes, amines, and ammonium sulfate, *Environ. Sci. Technol.*, *48*(24), 14,417–14,425, doi:10.1021/es5044479.

Gaston, C. J., T. P. Riedel, Z. Zhang, A. Gold, J. D. Surratt, and J. A. Thornton (2014), Reactive uptake of an isoprene-derived epoxydiol to submicron aerosol particles, *Environ. Sci. Technol.*, *48*(19), 11,178–11,186, doi:10.1021/es5034266.

Hennigan, C. J., M. H. Bergin, J. E. Dibb, and R. J. Weber (2008), Enhanced secondary organic aerosol formation due to water uptake by fine particles, *Geophys. Res. Lett.*, *35*, L18801, doi:10.1029/2008GL035046.

Hennigan, C. J., M. H. Bergin, A. G. Russell, A. Nenes, and R. J. Weber (2009), Gas/particle partitioning of water-soluble organic aerosol in Atlanta, *Atmos. Chem. Phys.*, *9*(11), 3613–3628, doi:10.5194/acp-9-3613-2009.

Hinds, W. C. (1999), *Aerosol Technology: Properties, Behavior, and Measurement of Airborne Particles*, 2nd ed., John Wiley, Hoboken, N. J.

Hodas, N., A. Zuend, W. Mui, R. C. Flagan, and J. H. Seinfeld (2015), Influence of particle-phase state on the hygroscopic behavior of mixed organic–inorganic aerosols, *Atmos. Chem. Phys.*, *15*, 5027–5045, doi:10.5194/acp-15-5027-2015.

Hodzic, A., B. Aumont, C. Knote, J. Lee-Taylor, S. Madronich, and G. Tyndall (2014), Volatility dependence of Henry's law constants of condensable organics: Application to estimate depositional loss of secondary organic aerosols, *Geophys. Res. Lett.*, *41*, 4795–4804, doi:10.1002/2014GL060649.

Hudman, R. C., L. T. Murray, D. J. Jacob, D. B. Millet, S. Turquety, S. Wu, D. R. Blake, A. H. Goldstein, J. Holloway, and G. W. Sachse (2008), Biogenic versus anthropogenic sources of CO in the United States, *Geophys. Res. Lett.*, *35*, L04801, doi:10.1029/2007GL032393.

Khlystov, A., C. O. Stanier, S. Takahama, and S. N. Pandis (2005), Water content of ambient aerosol during the Pittsburgh Air Quality Study, *J. Geophys. Res.*, *110*, D07S10, doi:10.1029/2004JD004651.

Kondo, Y., Y. Miyazaki, N. Takegawa, T. Miyakawa, R. J. Weber, J. L. Jimenez, Q. Zhang, and D. R. Worsnop (2007), Oxygenated and water-soluble organic aerosols in Tokyo, *J. Geophys. Res.*, *112*, D01203, doi:10.1029/2006JD007056.

Kroll, J. H., N. L. Ng, S. M. Murphy, V. Varutbangkul, R. C. Flagan, and J. H. Seinfeld (2005), Chamber studies of secondary organic aerosol growth by reactive uptake of simple carbonyl compounds, *J. Geophys. Res.*, *110*, D23207, doi:10.1029/2005JD006004.

Laskin, A., R. C. Moffet, M. K. Gilles, J. D. Fast, R. A. Zaveri, B. Wang, P. Nigge, and J. Shutthanandan (2012), Tropospheric chemistry of internally mixed sea salt and organic particles: Surprising reactivity of NaCl with weak organic acids, *J. Geophys. Res.*, *117*, D15302, doi:10.1029/2012JD017743.

Lee, A. K. Y., R. Zhao, R. Li, J. Liggio, S.-M. Li, and J. P. D. Abbatt (2013), Formation of light absorbing organo-nitrogen species from evaporation of droplets containing glyoxal and ammonium sulfate, *Environ. Sci. Technol.*, *47*(22), 12,819–12,826, doi:10.1021/es402687w.

Liggio, J., S. M. Li, and R. Mclaren (2005a), Heterogeneous reactions of glyoxal on particulate matter: Identification of acetals and sulfate esters, *Environ. Sci. Technol.*, *39*(6), 1532–1541, doi:10.1021/Es048375y.

Liggio, J., S. M. Li, and R. Mclaren (2005b), Reactive uptake of glyoxal by particulate matter, *J. Geophys. Res.*, *110*, D10304, doi:10.1029/2004JD005113.

Lim, Y. B., Y. Tan, M. J. Perri, S. P. Seitzinger, and B. J. Turpin (2010), Aqueous chemistry and its role in secondary organic aerosol (SOA) formation, *Atmos. Chem. Phys.*, *10*(21), 10,521–10,539, doi:10.5194/acp-10-10521-2010.

Lim, Y. B., Y. Tan, and B. J. Turpin (2013), Chemical insights, explicit chemistry, and yields of secondary organic aerosol from OH radical oxidation of methylglyoxal and glyoxal in the aqueous phase, *Atmos. Chem. Phys.*, *13*, 8651–8667, doi:10.5194/acp-13-8651-2013.

Lin, G., J. E. Penner, S. Sillman, D. Taraborrelli, and J. Lelieveld (2012), Global modeling of SOA formation from dicarbonyls, epoxides, organic nitrates and peroxides, *Atmos. Chem. Phys.*, *12*(10), 4743–4774, doi:10.5194/acp-12-4743-2012.

Lin, G., S. Sillman, J. E. Penner, and A. Ito (2014), Global modeling of SOA: The use of different mechanisms for aqueous-phase formation, *Atmos. Chem. Phys.*, *14*(11), 5451–5475, doi:10.5194/acp-14-5451-2014.

Loeffler, K. W., C. A. Koehler, N. M. Paul, and D. O. De Haan (2006), Oligomer formation in evaporating aqueous glyoxal and methyl glyoxal solutions, *Environ. Sci. Technol.*, *40*(20), 6318–6323, doi:10.1021/Es060810w.

Malm, W. C., and D. E. Day (2001), Estimates of aerosol species scattering characteristics as a function of relative humidity, *Atmos. Environ.*, *35*, 2845–2860.

McNeill, V. F. (2015), Aqueous organic chemistry in the atmosphere: Sources and chemical processing of organic aerosols, *Environ. Sci. Technol.*, *49*(3), 1237–1244, doi:10.1021/es5043707.

McNeill, V. F., J. L. Woo, D. D. Kim, A. N. Schwier, N. J. Wannell, A. J. Sumner, and J. M. Barakat (2012), Aqueous-phase secondary organic aerosol and organosulfate formation in atmospheric aerosols: A modeling study, *Environ. Sci. Technol.*, *46*(15), 8075–8081, doi:10.1021/Es3002986.

Miyazaki, Y., Y. Kondo, N. Takegawa, Y. Komazaki, M. Fukuda, K. Kawamura, M. Mochida, K. Okuzawa, and R. J. Weber (2006), Time-resolved measurements of water-soluble organic carbon in Tokyo, *J. Geophys. Res.*, *111*, D23206, doi:10.1029/2006JD007125.

Müller, J. F., T. Stavrakou, S. Wallens, I. De Smedt, M. Van Roozendael, M. J. Potosnak, J. Rinne, B. Munger, A. Goldstein, and A. B. Guenther (2008), Global isoprene emissions estimated using MEGAN, ECMWF analyses and a detailed canopy environment model, *Atmos. Chem. Phys.*, *8*(5), 1329–1341, doi:10.5194/acp-8-1329-2008.

Nguyen, T. B., P. B. Lee, K. M. Updyke, D. L. Bones, J. Laskin, A. Laskin, and S. A. Nizkorodov (2012), Formation of nitrogen- and sulfur-containing light-absorbing compounds accelerated by evaporation of water from secondary organic aerosols, *J. Geophys. Res.*, *117*, D01207, doi:10.1029/2011JD016944.

Nguyen, T. B., M. M. Coggon, K. H. Bates, X. Zhang, R. H. Schwantes, K. A. Schilling, C. L. Loza, R. C. Flagan, P. O. Wennberg, and J. H. Seinfeld (2014), Organic aerosol formation from the reactive uptake of isoprene epoxydiols (IEPOX) onto non-acidified inorganic seeds, *Atmos. Chem. Phys.*, *14*, 3497–3510, doi:10.5194/acp-14-3497-2014.

Nguyen, T. K. V., M. D. Petters, S. R. Suda, H. Guo, R. J. Weber, and A. G. Carlton (2014), Trends in particle-phase liquid water during the Southern Oxidant and Aerosol Study, *Atmos. Chem. Phys.*, *14*(20), 10,911–10,930, doi:10.5194/acp-14-10911-2014.

Ortiz-Montalvo, D. L., Y. B. Lim, M. J. Perri, S. P. Seitzinger, and B. J. Turpin (2012), Volatility and yield of glycolaldehyde SOA formed through aqueous photochemistry and droplet evaporation, *Aerosol Sci. Technol.*, *46*(9), 1002–1014, doi:10.1080/02786826.2012.686676.

Ortiz-Montalvo, D. L., S. A. Häkkinen, A. N. Schwier, Y. B. Lim, V. F. McNeill, and B. J. Turpin (2014), Ammonium addition (and aerosol pH) has a dramatic impact on the volatility and yield of glyoxal secondary organic aerosol, *Environ. Sci. Technol.*, *48*(1), 255–262, doi:10.1021/es4035667.

Paciga, A. L., I. Riipinen, and S. N. Pandis (2014), Effect of ammonia on the volatility of organic diacids, *Environ. Sci. Technol.*, *48*(23), 13,769–13,775, doi:10.1021/es5037805.

Paulot, F., J. D. Crounse, H. G. Kjaergaard, A. Kürten, J. M. S. Clair, J. H. Seinfeld, and P. O. Wennberg (2009), Unexpected epoxide formation in the gas-phase photooxidation of isoprene, *Science*, *325*(5941), 730–733, doi:10.1126/science.1172910.

Powelson, M. H., B. M. Espelien, L. N. Hawkins, M. M. Galloway, and D. O. De Haan (2014), Brown carbon formation by aqueous-phase carbonyl compound reactions with amines and ammonium sulfate, *Environ. Sci. Technol.*, *48*(2), 985–993, doi:10.1021/es4038325.

Pruppacher, H. R. (1986), The role of cloudphysics in atmospheric multiphase systems: Ten basic statements, in *Chemistry of Multiphase Atmospheric Systems*, edited by W. Jaeschke, pp. 133–190, Springer, New York.

Pye, H. O. T., et al. (2013), Epoxide pathways improve model predictions of isoprene markers and reveal key role of acidity in aerosol formation, *Environ. Sci. Technol.*, *47*(19), 11,056–11,064, doi:10.1021/es402106h.

Renbaum-Wolff, L., J. W. Grayson, A. P. Bateman, M. Kuwata, M. Sellier, B. J. Murray, J. E. Shilling, S. T. Martin, and A. K. Bertram (2013), Viscosity of α-pinene secondary organic material and implications for particle growth and reactivity, *Proc. Natl. Acad. Sci. U.S.A.*, *110*(20), 8014–8019, doi:10.1073/pnas.1219548110.

Riedel, T. P., Y. H. Li, S. H. Budisulistiorini, C. J. Gaston, J. A. Thornton, Z. Zhang, W. Vizuete, A. Gold, and J. D. Surratt (2015), Heterogeneous reactions of isoprene-derived epoxides: Reaction probabilities and molar secondary organic aerosol yield estimates, *Environ. Sci. Technol. Lett.*, *2*(2), 38–42, doi:10.1021/ez500406f.

Sareen, N., A. N. Schwier, E. L. Shapiro, D. Mitroo, and V. F. McNeill (2010), Secondary organic material formed by methylglyoxal in aqueous aerosol mimics, *Atmos. Chem. Phys.*, *10*(3), 997–1016, doi:10.5194/acp-10-997-2010.

Shapiro, E. L., J. Szprengiel, N. Sareen, C. N. Jen, M. R. Giordano, and V. F. McNeill (2009), Light-absorbing secondary organic material formed by glyoxal in aqueous aerosol mimics, *Atmos. Chem. Phys.*, *9*(7), 2289–2300, doi:10.5194/acp-9-2289-2009.

Song, M., P. F. Liu, S. J. Hanna, Y. J. Li, S. T. Martin, and A. K. Bertram (2015), Relative humidity-dependent viscosities of isoprene-derived secondary organic material and atmospheric implications for isoprene-dominant forests, *Atmos. Chem. Phys.*, *15*, 5145–5159, doi:10.5194/acp-15-5145-2015.

Sorooshian, A., S. M. Murphy, S. Hersey, R. Bahreini, H. Jonsson, R. C. Flagan, and J. H. Seinfeld (2010), Constraining the contribution of organic acids and AMS *m/z* 44 to the organic aerosol budget: On the importance of meteorology, aerosol hygroscopicity, and region, *Geophys. Res. Lett.*, *37*, L21807, doi:10.1029/2010GL044951.

Sullivan, A. P., R. E. Peltier, C. A. Brock, J. A. de Gouw, J. S. Holloway, C. Warneke, A. G. Wollny, and R. J. Weber (2006), Airborne measurements of carbonaceous aerosol soluble in water over northeastern United States: Method development and an investigation into water-soluble organic carbon sources, *J. Geophys. Res.*, *111*, D23S46, doi:10.1029/2006JD007072.

Surratt, J. D., M. Lewandowski, J. H. Offenberg, M. Jaoui, T. E. Kleindienst, E. O. Edney, and J. H. Seinfeld (2007), Effect of acidity on secondary organic aerosol formation from isoprene, *Environ. Sci. Technol.*, *41*(15), 5363–5369, doi:10.1021/Es0704176.

Tan, Y., M. J. Perri, S. P. Seitzinger, and B. J. Turpin (2009), Effects of precursor concentration and acidic sulfate in aqueous glyoxal-OH radical oxidation and implications for secondary organic aerosol, *Environ. Sci. Technol.*, *43*(21), 8105–8112, doi:10.1021/Es901742f.

Volkamer, R., F. S. Martini, L. T. Molina, D. Salcedo, J. L. Jimenez, and M. J. Molina (2007), A missing sink for gas-phase glyoxal in Mexico City: Formation of secondary organic aerosol, *Geophys. Res. Lett.*, *34*, L19807, doi:10.1029/2007GL030752.

Volkamer, R., P. J. Ziemann, and M. J. Molina (2009), Secondary organic aerosol formation from acetylene (C_2H_2): Seed effect on SOA yields due to organic photochemistry in the aerosol aqueous phase, *Atmos. Chem. Phys.*, *9*(6), 1907–1928, doi:10.5194/acp-9-1907-2009.

Wang, B., and A. Laskin (2014), Reactions between water-soluble organic acids and nitrates in atmospheric aerosols: Recycling of nitric acid and formation of organic salts, *J. Geophys. Res. Atmos.*, *119*, 3335–3351, doi:10.1002/2013JD021169.

Weber, R. J., et al. (2007), A study of secondary organic aerosol formation in the anthropogenic-influenced southeastern United States, *J. Geophys.*, *112*, D13302, doi:10.1029/2007JD008408.

Yli-Juuti, T., et al. (2013), Volatility of organic aerosol: Evaporation of ammonium sulfate/succinic acid aqueous solution droplets, *Environ. Sci. Technol.*, *47*(21), 12,123–12,130, doi:10.1021/es401233c.

You, Y., et al. (2012), Images reveal that atmospheric particles can undergo liquid-liquid phase separations, *Proc. Natl. Acad. Sci. U.S.A.*, *109*(33), 13,188–13,193, doi:10.1073/pnas.1206414109.

Yu, G., A. R. Bayer, M. M. Galloway, K. J. Korshavn, C. G. Fry, and F. N. Keutsch (2011), Glyoxal in aqueous ammonium sulfate solutions: Products, kinetics and hydration effects, *Environ. Sci. Technol.*, *45*(15), 6336–6342, doi:10.1021/es200989n.

Yuan, B., et al. (2015), Investigation of secondary formation of formic acid: Urban environment vs. oil and gas producing region, *Atmos. Chem. Phys.*, *15*, 1975–1993, doi:10.5194/acp-15-1975-2015.

Zhang, X., et al. (2012), On the gas-particle partitioning of soluble organic aerosol in two urban atmospheres with contrasting emissions: 1. Bulk water-soluble organic carbon, *J. Geophys. Res.*, *117*, D00V16, doi:10.1029/2012JD017908.